Open Access

Journal of Energy and Power Technology

LIDSEN Publishing Inc.

Research Article

Controller Evaluation for Solar-Latent Thermal Energy Applications

John Konstantaras [1], Christos Pagkalos [1], Maria K. Koukou [1,*], Kostas Lymperis [1], Yannis Caouris [2], Michail Gr. Vrachopoulos [1]

1. National and Kapodistrian University of Athens, Department of Agricultural Development, Agrofood and Management of Natural Resources, Energy and Environmental Research Laboratory, Psachna Campus, 34400 Evia, Greece; E-Mails: yiannis.konstantaras@gmail.com; pagkalos.christos@gmail.com; mkoukou@uoa.gr; lymperiskostas@gmail.com; mgrvrachop@uoa.gr
2. University of Patras, Department of Mechanical Engineering & Aeronautics, 26504 Rio Achaia, Greece; E-Mail: caouris@upatras.gr

* **Correspondence:** Maria K. Koukou; E-Mail: mkoukou@uoa.gr

Academic Editor: Mariano Alarcón

Special Issue: Solar Thermal Energy

Journal of Energy and Power Technology
2022, volume 4, issue 2
doi:10.21926/jept.2202021

Received: April 17, 2022
Accepted: May 31, 2022
Published: June 09, 2022

Abstract

In this study, the performance of a self-sufficient controller used for a solar-latent heat domestic hot water (DHW) production unit under real-world operating conditions was analyzed. The unit consists of a flat-plate solar collector and a latent heat storage tank. The controller is powered by a small solar panel and governs the charging and discharging of the system, ensuring maximum solar energy absorption, desired hot water temperature, and constant monitoring of the heat-storage tank's capacity. The system is compact and can be installed on flat and curved roofs as a direct replacement of conventional solar collectors with heat-energy storage tanks. During testing, all internal and external parameters were monitored using a monitoring system that was also used for emulating user profiles. The controller uses self-learning techniques to adjust its parameters and improves its performance by fine-tuning the control equations to the peculiarities of the specific system and installation

location. The system was installed and operated for an extended period to allow for the learning equations to train the system. The results for the first, fifth, and twentieth days of operation are presented in this paper. On the 20th operating day, the controller effectively regulated the heat transfer fluid temperature difference in the charging circuit within the efficient band of 2°C–5°C following the irradiance conditions at the testing area. During discharge, the DHW temperature was regulated between 37°C–40°C, with the user's set temperature as 38°C. The regulation hysteresis time for the DHW temperature regulation was approximately 5 min. The tests were conducted under real-world operating conditions for the charging of the system, while for the discharging, the user profile was emulated using a test rig.

Keywords
Solar thermal system; domestic hot water; latent heat storage; phase-change materials; self-learning controller

1. Introduction

Solar thermal applications incorporating latent heat storage have grown in popularly both at the research and application levels in recent years [1-5]. In addition to the use of solar thermal energy storage in phase change materials (PCMs) to meet thermal energy needs, latent heat storage can be used to improve the efficiency of other energy systems such as photovoltaic (PV) power generation [6-9]. The intermittency and unpredictability of solar radiation as an energy source and the nonlinear relationship between energy storage medium temperature and stored energy that governs latent heat storage applications necessitate the use of advanced methods for the controlled operation of such units. Abdelsalam et al. [10] developed a numerical model to compare solar thermal systems and found that the use of PCMs in solar thermal energy storage tanks can help reduce the volume of the tank by 40%. They also noted a considerable increase (as high as 23%) in the solar fraction in systems with direct heat exchangers (HEs) as compared with those with indirect HEs. However, the current study focused on hybrid (water–PCM) storage tanks wherein the storage tank was filled 100%, making the direct HE solution more complicated.

Controllers are an essential component of solar thermal systems and help increase energy efficiency and enhance user safety and user experience. Various solar thermal control strategies have been proposed. Andrade et al. [11] highlighted the nonlinear dynamics of solar plants that inhibit the performance of linear controllers. They simulated and tested two nonlinear controllers in a solar plant and evaluated their performance in terms of tracking and disturbance rejection. Both controllers exhibited promising results and better performance than a classic PI controller. The current study aimed to achieve comparable results by using linear controllers incorporating simple training algorithms to enhance the performance of the system. Badescu [12, 13] investigated the most effective strategies for flow control in solar collectors aiming for maximum exergy extraction.

Another important function of a controller in a solar thermal system is system protection and fault prevention. Elias et al. [14] used a hybrid predictive control function to prevent overheating of

the heat transfer fluid (HTF) in solar systems. Overheating is an issue in solar systems because it raises safety concerns.

Víg et al. [15] investigated the evolution of energy characteristics in domestic vacuum tube solar collectors and noted that HTF flow control increased the efficiency of the system by up to 13%. This effect is more pronounced on overcast days or when the thermal energy storage tank is almost full. Araújo et al. [16-18] investigated the effects of on/off control and proportional flow rate control in solar thermal systems and noted an increase in solar fraction by up to 50% upon the use of proportional control. Furthermore, proportional control exhibits increased efficiency when the water storage tank volume is increased as opposed to on/off control, wherein the efficiency remains constant or decreases when the storage tank volume is increased.

Although controllers for solar thermal systems have been extensively studied, the concept of a solar collector coupled with a PCM tank is fairly new. Such systems require well-designed control routines due to the low heat capacity of the fluid in the charging loop (because the required volume is decreased). In addition, such systems can easily get overheated and render the PCM useless due to chemical decomposition at temperatures higher than the stipulated operating temperatures. Hot-water production in such systems is also challenging because the hot water is not stored in the tank but is instantly produced when needed. Temperature regulation of the produced hot water is essential to enhance user safety and increase energy efficiency.

Tourou et al. [19] employed proportional flow control in latent thermal energy units and achieved promising results. They used an emulation platform to perform tests under different operating conditions at the laboratory scale and in a controlled environment.

In the current study, the performance of the controller was investigated for the efficient operation of a solar kit unit [20] comprising an innovative solar collector integrated with thermal energy storage. The unit was designed and simulated for various conditions [21]. The results of the simulations were used for the development of true-scale prototype units, which were then evaluated under real-world operating (outdoors) conditions, and their performance characteristics were measured before the installation of the controller [20]. The roof of the university campus at Psachna, Evia, Greece, was used as the test area, and the tests were conducted between September 3 and 23, 2020. The area has a typical Mediterranean climate; the summers are hot and dry, and in winters, there is a lot of rain and humidity. The problem of overheating is more significant in latent solar thermal systems than in conventional heat solar thermal systems because of the chemical instability that PCMs exhibit at temperatures over their operating limit. The controller designed in the present work employs system protection routines to secure the system against overheating and freezing. The test results after the installation of the controller are presented in Section 3.

2. Materials and Methods

The solar kit unit (Figure 1) comprises a solar collector and a PCM storage tank installed on the back of the collector. The PCM storage tank is a stainless-steel tank with a fin and tube HE immersed in it. The dimensions of the tank are 2006 mm × 997 mm × 88 mm, and its net volume is 338 L. For the thermal insulation of the tank, an 80-mm-thick layer of rock wool insulation was used. Finally, for the protection of the insulation, the tank was wrapped with a 0.6-mm-thick aluminum layer. Commercial paraffin wax was used as the latent heat storage medium, with a phase change temperature of 53°C. The total mass of the PCM used is 140 kg.

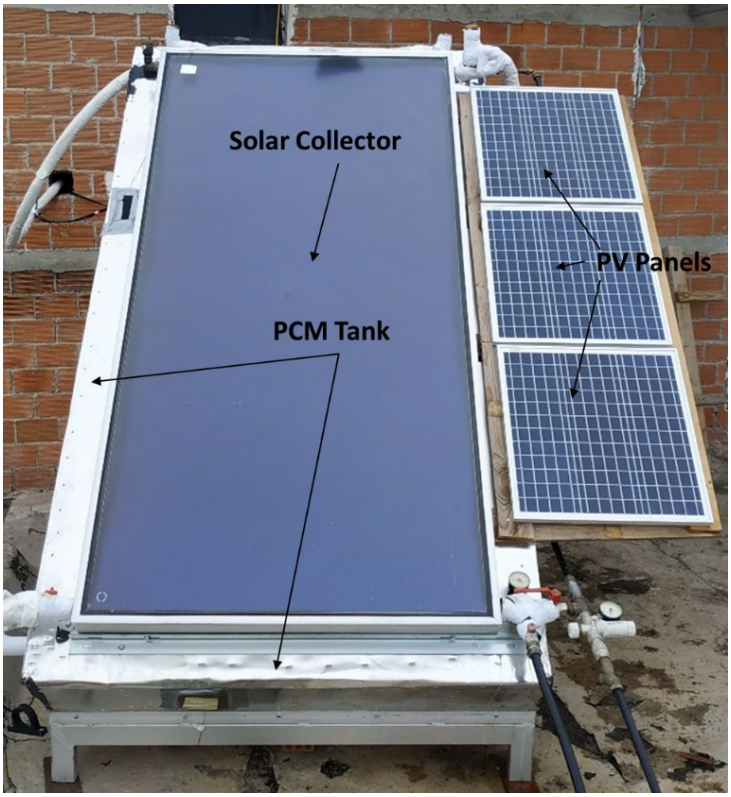

Figure 1 The solar kit unit containing a solar collector, a PCM tank, and PV panels.

The HE (Figure 2) immersed in the PCM tank has two circuits. The first circuit is hydraulically connected to the solar collector and is responsible for heat transfer between the solar collector and the PCM (through the HTF). The HTF in this loop is circulated using a circulation pump (CP1 in Figure 3) that is commanded by the controller to ensure maximum solar energy absorption by the system. The second circuit of the HE is connected in an open loop. The inlet to the HE is connected to the tap water supply, and the output of the HE is connected to the domestic hot water (DHW) network of the building. An analog three-way mixing valve (VC1 in Figure 3) is placed between the HE outlet and the DHW supply and is used to mix the hot water at the outlet of the HE with cold tap water to achieve the ideal DHW temperature. This valve is also commanded by the controller. For the circulation of the water in the open loop, no pump is used because the pressure of the tap water network is utilized like in an ordinary solar collector. The HE has 417 aluminum fins that are used for the energy transfer between the HE circuit and the PCM; the fins are necessary to improve heat transfer due to the low thermal conductivity of the paraffin-based PCM.

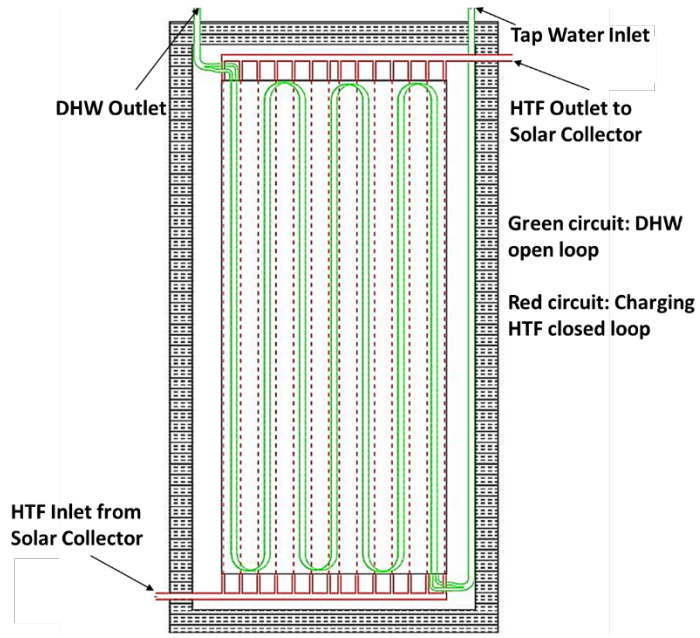

Figure 2 Schematic of the HE showing the two circuits.

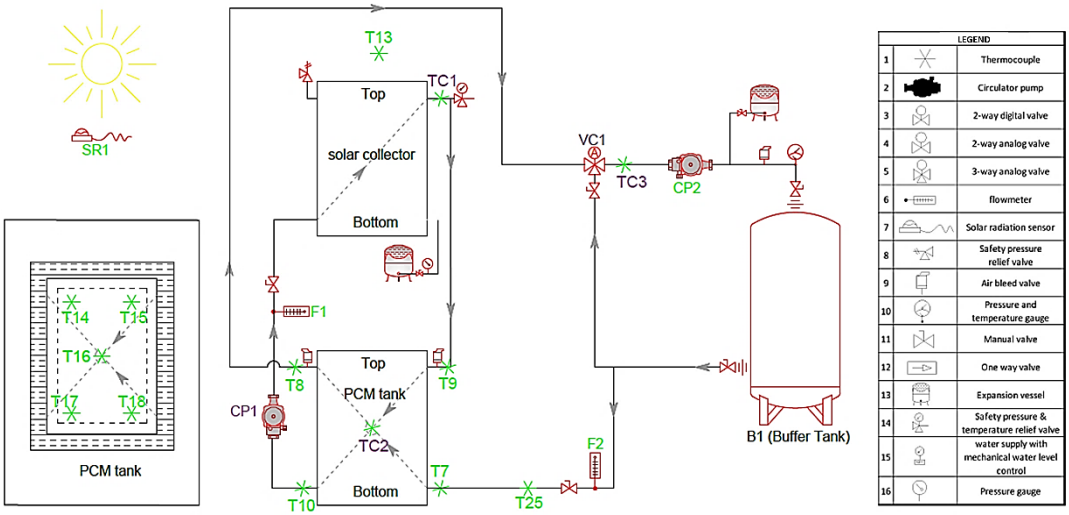

Figure 3 Hydraulic scheme of the setup.

For testing the controller under real-world operating conditions, a full-scale setup was used (Figure 3). The system can be divided into two main sections according to the energy flow. The charging loop consists of the flat-plate solar collector that absorbs energy from solar radiation and converts it to heat, increasing the temperature of the HTF. The HTF was circulated using a small solar-powered circulation pump placed between the solar collector and the latent heat storage PCM tank. This part of the testing circuit is identical to the one designed for practical applications. The discharging loop includes the second circuit of the HE, the three-way mixing valve, and the buffer (B1 in Figure 3). The buffer was cooled by an external chiller and was used to simulate tap water temperature. The CP2 (Figure 3) circulation pump was also used in the discharging loop to simulate tap water pressure. The sensors and actuators used in the test rig to emulate the test conditions and measure the performance of the system are presented in Table 1 along with their operating characteristics.

Table 1 Specifications of the sensors and actuators used in the test setup.

	Type	Range	Accuracy	Supply Characteristics	Communication Signal
Thermocouples	T type	−270 °C–370°C	±0.5°C	-	Thermocouple
Flow Meters	Oval Gear	0.8–8.3 L/min	±5%	24 VDC	4–20 mA
Pyranometer	Thermopile Detector	20–2000 W/m^2	ISO 9060 First Class	24 VDC	4–20 mA
Digital Valves	Servo-mechanical actuator	ON/OFF	-	24 VDC	24 VDC
Analog Valves	Servo-mechanical actuator	0–90°/90S	±5%	24 VDC	2–10 VDC

The control system comprises the main controller (Siemens Logo ® PLC), sensors, and actuators and is shown in Figure 4 while the control logic is presented with a flowchart shown in Figure 5. The system is powered by two PV panels with a nominal voltage of 12 V and a power rating of 30 Wp. Two lead-acid batteries are used to power the system when the PV's power production is not sufficient. The battery bank has a nominal voltage of 24 V nominal and a capacity of 7 Ah. The control system is designed to use minimum power between sunset and sunrise and thus requires a small battery. For the tests, a separate 12-V/30-Wp solar panel was used to power the circulating pump. Nevertheless, the system has been designed to operate using a single 24-V/30-Wp solar panel to power all the devices, and this has been proven from the measurements of the state of charge of the battery bank, which never dropped below 80% during the testing period.

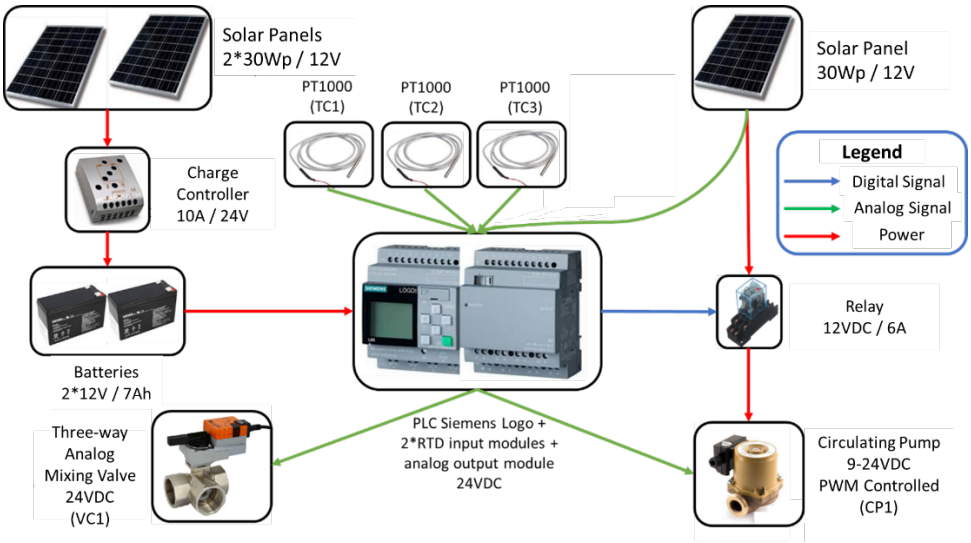

Figure 4 Controller connection scheme.

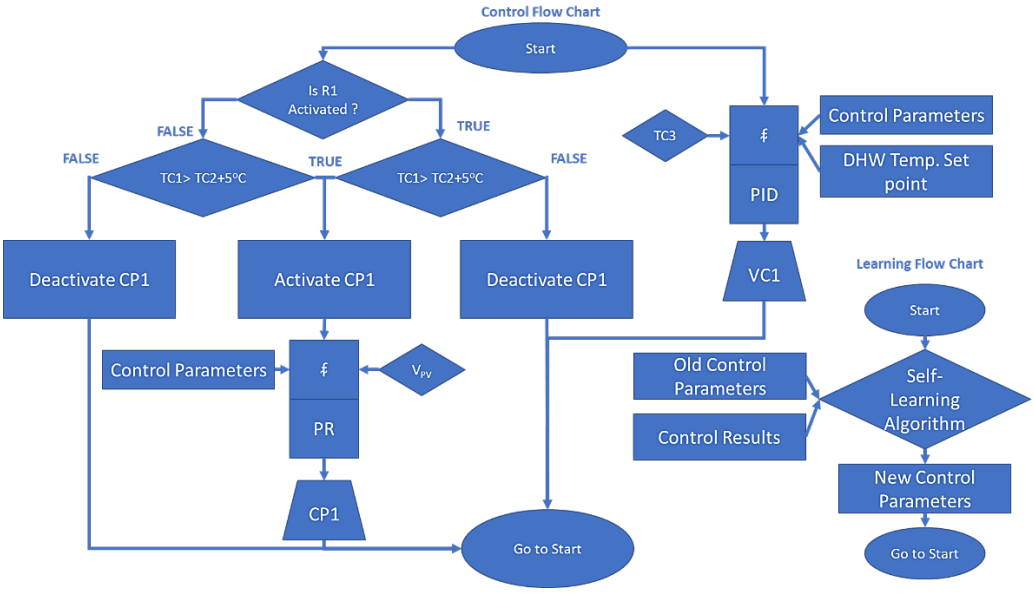

Figure 5 Flowchart of the controller operation.

Three PT1000 temperature sensors were used to measure the temperature at the outlet of the solar collector (TC1), the temperature of the PCM in the tank (TC2), and the temperature of the DHW at the outlet of the three-way mixing valve (TC3). The voltage of the systemwas monitored to calculate the charge state of the battery and take decisions to reduce the measuring and control frequency of the controller to save power when the battery charge was low and to decide when to put the controller into "sleep mode" when the battery was close to empty. The PV voltage with the panel disconnected from the battery was used as an inexpensive solar radiation sensor. An equation was formulated for converting the PV's open-circuit voltage into solar radiation energy per unit area, and the obtained value was then fed to the controller's charging control loop to decide the state of operation of the charging circulation pump.

24-VDC actuators were used so as to be powered directly from the battery bank of the system and use low power. The circulating pump was used to circulate the HTF between the solar collector and the HE charging circuit. The pump was controlled by the PLC by using pulse width modulation (PWM) control, and a relay was used to isolate the pump from the power system when there was no need for HTF circulation. The three-way mixing valve was also 24-VDC powered and was used to mix cold tap water with the water at the outlet of the HE to produce DHW at a constant temperature to satisfy the user's requirements and prevent injury from extremely hot DHW. This valve is essential for the operation of the system because the temperature at the outlet of the HE depends on the state of charge of the PCM tank, the tap water temperature, and the flow rate of the water in the DHW network of the building and thus fluctuates greatly. The controller was used to monitor the temperature at the outlet of the three-way valve and adjust it to stabilize the DHW temperature at the desired level regardless of the affecting parameters described. The specifications of the sensors and actuators used in the control system are presented in Table 2. Efforts were made to optimize control component costs without compromising the controller's effectiveness.

Table 2 Specifications of the sensors and actuators used in the controller.

	Type	Range	Accuracy	Supply Characteristics	Communication Signal
Temperature Sensors	PT1000	−50 °C–150°C	±(0.15°C + 0.2%) (Class A)	4 Wire Setup Current Driven	4 Wire Setup Voltage Output
Analog Valves	Servo-mechanical actuator	0–90°/90 S	±5%	24 VDC	2–10 VDC
Pyranometer	Photovoltaic Cell	0–1000 W/m^2	Custom Sensor (Internal Calibration)±5%		0–24 VDC

The setup was tested under real-world operating conditions. The system was mounted on the roof of building D in the Evripus building complex of the National and Kapodistrian University of Athens at Psachna, Evia, Greece, and was monitored using an external monitoring platform by using LabView® software. The user profile was emulated using the monitoring platform. An emulation rig was used for the tests. The setup is shown in Figure 1. For the tests, the parameters presented in Table 3 were used:

Table 3 Parameters for the testing procedures.

End Charging PCM Temperature (°C)	70
End Charging Solar Radiation (W/m^2)	68
Discharging Water Flow (L/h)	100
End Discharging Water Temperature (°C)	38
DHW Temperature Set-point	38
Tap Water Temperature (°C)	15

The testing procedure consisted of more than 30 testing cycles, but in this paper, cycles 1, 5, and 20 are presented to show the effect of self-training on the effectiveness of the controller. Each cycle was divided into the charging and discharging phases and was completed within a day. The emulation platform was used to monitor all internal and external parameters of the system, namely solar radiation, ambient temperature, the temperature at various points of the hydraulic circuits, the temperature inside the PCM tank, and the volumetric flow of the HTF in the charging loop and that of the water in the discharging loop.

Each testing cycle started with the charging phase at dawn. When the temperature of the HTF at the outlet of the solar collector satisfied the pump starting criteria of the controller, the circulation pump was activated. The operating point of the pump was adjusted via PWM by using a self-learning algorithm that also considers the temperature of the PCM inside the tank and the temperature of the HTF at the outlet of the solar collector. The pump operating point was adjusted to achieve maximum solar power absorption by the system, and the pump could be turned off by the controller for some time if required. This operation was continued until dusk or stopped when the PCM tank temperature exceeded the fully charged limit.

After the charging, the discharging phase was automatically started by the monitoring and emulation platform. Generally, this phase starts when the user needs DHW, but for the purpose of the tests, it started automatically after charging and continued uninterrupted until the PCM tank was completely discharged. During this phase, the controller monitored the temperature at the outlet of the three-way valve and adjusted it to achieve a DHW temperature equal to the specified value.

The self-learning algorithm continuously monitored the system's operating conditions by monitoring the input parameters (i.e., the temperature of the tap water and the solar irradiance in the area). The system state was determined by measuring the HTF temperature, the operating state of the circulating pump, and the operating point of the three-way mixing valve. Lastly, the system's performance was determined by measuring the DHW temperature and PCM temperature. The controller uses this information, links the input parameters, system state, and system performance for each given time frame; and stores this information in a table together with the control equation coefficients used at the particular time frame. Because the objective of the controller is known (i.e., maximum solar absorption and DHW production at the temperature set by the user), the self-learning routine "promotes" the control equation coefficients that achieve better results by storing them in the upper rows of the table. Furthermore, the table entries that yield poor system performance are "demoted" to the lower rows of the table. This constitutes the self-learning part of the system. The controller operates by using the control coefficients that are stored at the first line of the table that has input and state parameters close to the actual measurements for each "decision" time.

The controller was tested for several cycles to determine its effectiveness when the algorithm is not trained and after a few cycles when the self-learning loop has manipulated the parameters of the controller (learning procedure). The results of these tests are presented in Section 3.

3. Results and Discussion

3.1 Untrained Controller on the First Day of Operation

3.1.1 Performance of the Controller During the Charging Cycle

The control behavior of the system during the charging cycle with no training is discussed here. Because the training algorithm has no data for training the controller, the behavior of the controller is assumed to be similar to that of a simple proportional controller.

The flow of the HTF in the charging loop during the charging cycle on the first day of operation is illustrated in In Figure 6; the incident solar radiation curve for the same day as measured on-site is also shown. The results revealed that the untrained controller does not respond to the changes in the incident solar radiation; thus, the charging flow remains almost constant during the entire charging cycle. Moreover, the controller yields no response during the times with partial clouding (t = 5.2 h, 7.5−8.4 h, and 8.8−10.6 h). Another effect of the poor performance of the controller is that during sunrise and sunset, the flow must be varied using the on/off strategy instead of proportional control. All these problems greatly reduce the performance of the system during charging because of the very fast changes in the HTF temperature at the inlet of the PCM tank that create temperature abnormalities in the PCM mass.

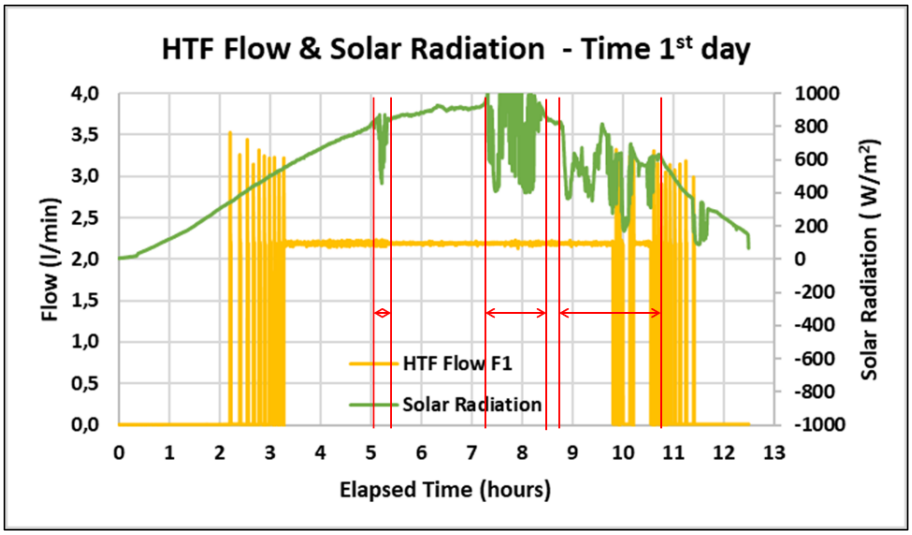

Figure 6 HTF flow rate and solar radiation versus time graph for the first day of operation.

In Figure 7, the temperatures of the HTF at the inlet and outlet of the PCM tank during the charging procedure and the average temperature of the PCM inside the tank are depicted. The control rule for the charging procedure is to maintain a low HTF temperature difference between the inlet and outlet of the PCM tank while ensuring efficient heat transfer from the solar collector to the PCM. This is essential because the HTF temperature at the outlet of the solar collector (inlet of the PCM tank) is critical for the efficiency (solar fraction) of the solar collector, which, in turn, greatly affects the overall efficiency of the system during charging. Because the controller is not trained and the circulating pump is operated in the on/off mode, the temperature at the inlet of the PCM tank greatly fluctuates, as seen in Figure 7 at t = 2.2−3.3 h, 9.8−10.2 h, and 10.6−11.4 h. During those time frames, the temperature of the HTF fluctuated by more than 12°C, thereby greatly inhibiting the solar fraction of the collector.

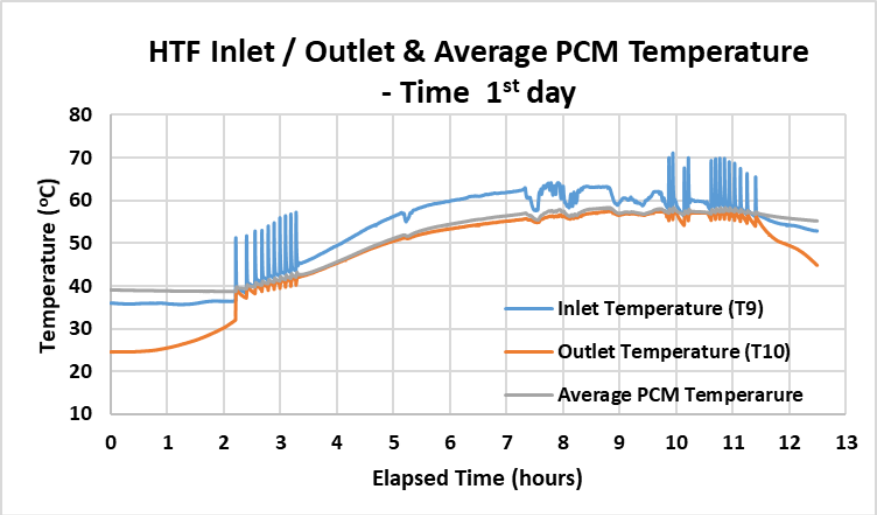

Figure 7 HTF inlet/outlet temperature and average PCM temperature versus time graph for the first day of operation.

3.1.2 Performance of the Controller During the Discharging Cycle

The temperature of the water at the inlet of the PCM tank (T7 in Figure 3), at the outlet of the tank (T8 in Figure 3), and the temperature of DHW (TC3 in Figure 3) during the discharging cycle for the first day of operation are shown in Figure 8. During the discharging cycle, the controller is mainly used to control the three-way mixing valve and produce DHW at a temperature set by the user. The temperature of the DHW must be maintained constant and equal to that set by the user regardless of the temperature of the tap water (inlet temperature) and the temperature of the PCM inside the tank. For the tests, the set-point for the DHW temperature was 38°C.

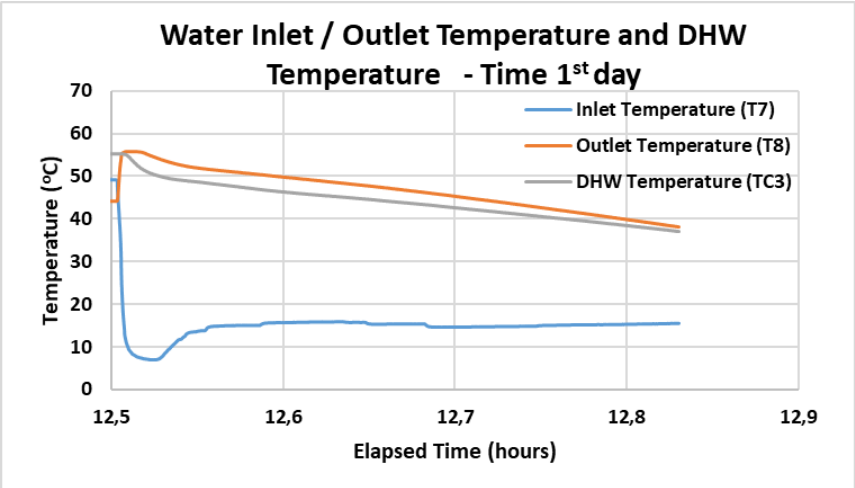

Figure 8 Water inlet/outlet and DHW temperature versus time graph for the first day of operation.

From the graph in Figure 8, it is obvious that the controller exhibits poor performance because it cannot maintain the DHW temperature constant. The temperature at the outlet of the tank decreases as the stored energy is consumed. This occurs due to the energy degradation of the PCM, resulting in undesirably high DHW temperatures that are unsafe for users when the tank is fully charged and very low temperatures when the tank is almost empty. The controller must be able to respond to this temperature change in a timely manner to ensure a constant DHW temperature that is as close to that set by the user as possible. Increasing the temperature of the DHW results in the wastage of the thermal energy of the tank as losses of the DHW network. Another issue with this configuration is that the user cannot effectively regulate the water temperature at the tap because of the continuous changes in the DHW temperature.

3.2 Partially Trained Controller on the Fifth Day of Operation

After four days of operation, the controller was considered to be partially trained. The training loop acquired sufficient data to be able to "understand" the dynamics of the system and use the collected measurements to improve the coefficients of the control equations by introducing Integral and derivative gains to the Proportional – Integral – Derivative controller. The gains are not expected to be fine-tuned yet because the operation of the system at this stage is governed by only proportional control.

3.2.1 Performance of the Controller During the Charging Cycle

The performance of the system during the fifth day of operation is discussed here. The training loop of the controller used the measurement results collected from the system on the previous four days and used them to improve the coefficients of the control equations.

The flow of the HTF in the charging loop and the solar irradiance in the area of the tests during the charging procedure on the fifth day of operation are shown in Figure 9; it can be seen that the controller responds to the normal change in the solar irradiance during the day and to partial clouding conditions (t = 6.7−7.2 h). However, during sunrise and sunset, the controller fails to respond proportionally to the change in the solar irradiance, and on/off control must be observed. The fifth day was chosen as it was a cloudy day (especially after midday). Cloudy conditions are challenging for any solar control system and thus ideal for performance evaluation.

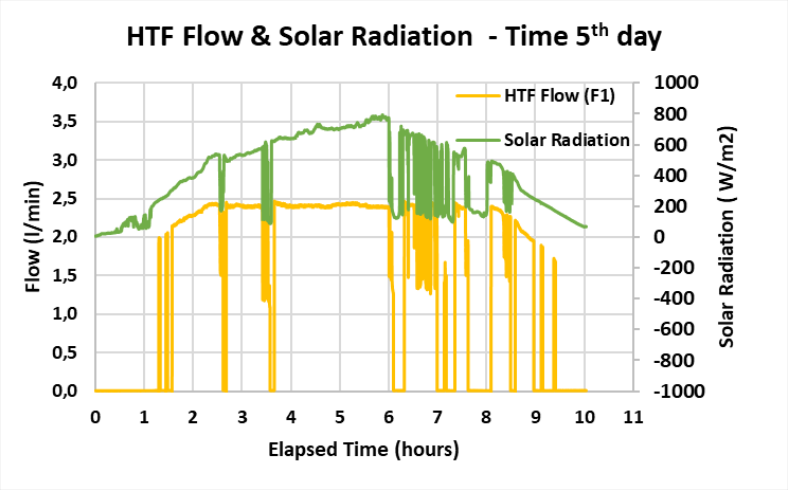

Figure 9 HTF Flow and Solar Radiation versus time graph for the fifth day of operation.

The performance of the thermal energy storage PCM tank on the fifth day of operation is shown in Figure 10. Although the controller utilized some training to increase its performance, poor handling of the clouding conditions was observed, resulting in an increased number (12) of on/off cycles for the HTF pump. At the beginning of those cycles, the HTF temperature fluctuated, and the performance of the systems deteriorated. After midday, when severe clouding was observed, the HTF temperatures fluctuated. In addition, the temperature difference between the outlet of the PCM tank and inside the tank was very high (higher than 7°C for the case of t = 8 h). The increased temperature difference between the HTF at the outlet and the PCM resulted in a very low flow rate, which decreased the efficiency of the charging cycle and created temperature inequalities inside the tank, resulting in a decrease in the thermal energy storage capacity of the PCM tank.

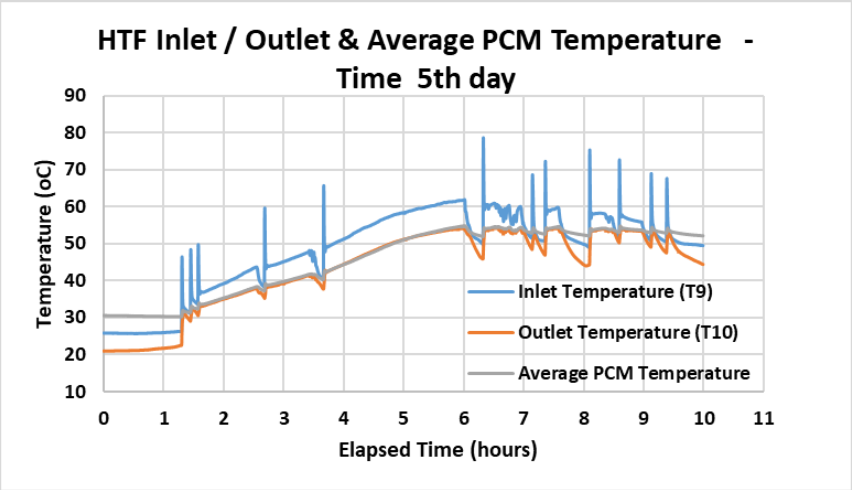

Figure 10 HTF inlet/outlet temperature and average PCM temperature versus time graph for the fifth day of operation.

3.2.2 Performance of the Controller During the Discharging Cycle

The response of the controller during discharging for the fifth day of operation is shown in Figure 11. The system responded well to normal temperature changes in the PCM tank and maintained a fairly constant DHW temperature. The average DHW temperature was near that set by the user except for the time frame of t = 10–10.06 h at the beginning of the discharge cycle when the controller cannot adequately respond to sudden changes in the temperature.

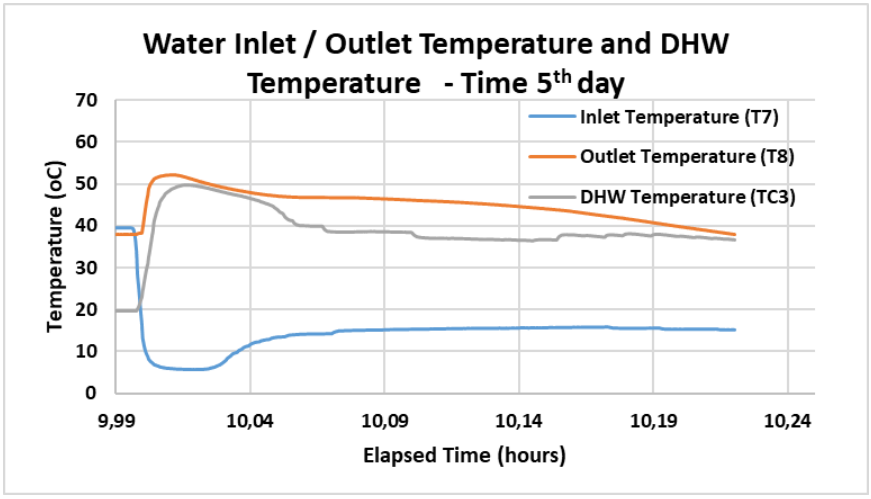

Figure 11 Water inlet/outlet and DHW temperature versus time graph for the fifth day of operation.

3.3 Well-trained Controller on the 20th Day of Operation

After 19 days of training, the controller was considered to be fully trained. During this stage, sufficient data were collected by the training routine to fully map the system dynamics and user behavior. This data is sufficient for fine-tuning the controller and achieving optimal performance. In addition, during the previous days, “abnormal” conditions such as sudden clouding, high DHW consumption, and sudden changes in tap water temperature must have occurred. The training

algorithm is expected to utilize these rare phenomena to further train the controller and enhance its ability to handle such rare events. After this stage, the training routine will continue to evaluate the performance of the system and improve the control equations, but the changes in the values of the parameters are expected to be minimal and rare.

3.3.1 Performance of the Controller During the Charging Cycle

The HTF flow and induced solar radiation during the charging cycle for the 20th day of operation are shown in Figure 12. The controller fully developed its ability to handle partial and fully overcast conditions with proportional control as observed at t = 3.99–4.04 h and 4.83–6.25 h, respectively. During these periods, the HTF temperature difference between the outlet of the tank and the average PCM temperature was kept minimal, as shown in Figure 13. This is the desired behavior as it eliminates temperature inequalities in the tank and increases the available storage capacity. At the end of the charging cycle (t = 8.25–9.60 h), the controller employs on/off control. During this time, the thermal energy storage tank is almost full, and the solar radiation is less. The pump speed cannot be set below the manufacturer's specified value; thus, the controller is forced to use on/off control to collect the solar energy available at the end of the day.

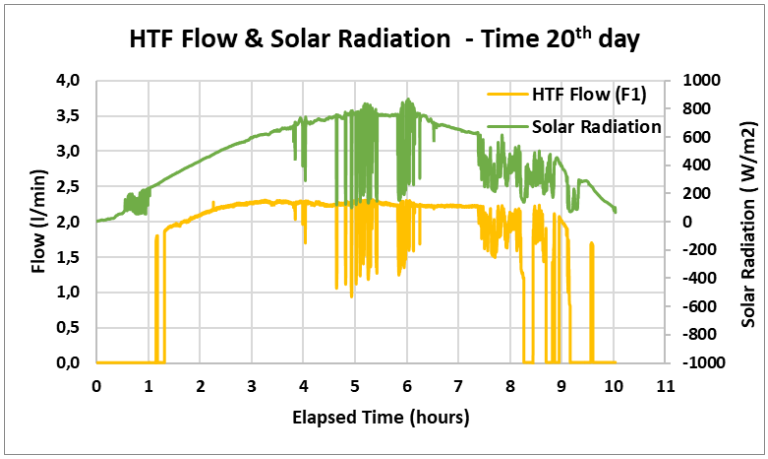

Figure 12 HTF Flow and Solar Radiation versus time graph for the 20th day of operation.

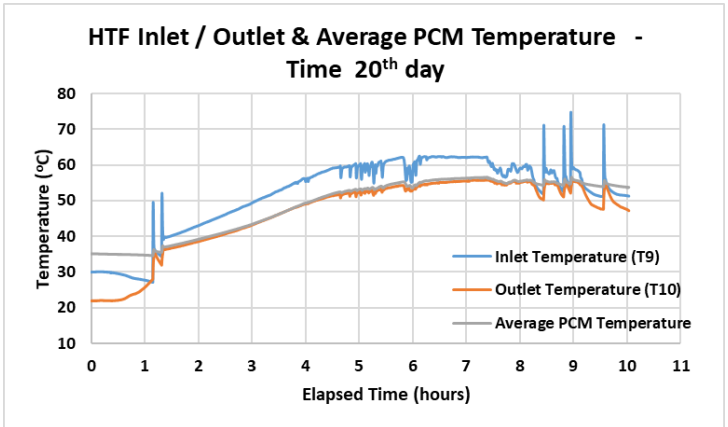

Figure 13 HTF inlet/outlet temperature and average PCM temperature versus time graph for the 20th day of operation.

3.3.2 Performance of the Controller During the Discharging Cycle

The performance of the system during discharging for the 20th day of operation is illustrated in Figure 14. The DHW temperature was maintained between 36°C and 40°C for the entire discharging cycle except for the start of the cycle (t = 9.85–9.90 h), when the DHW temperature was considerably higher than that set by the user (Table 3). The temperature at the start of each consumption cycle (when the user opens the tap) was not regulated regardless of the training stage of the controller. This is a very fast event that is beyond the capabilities of a linear controller; thus, a nonlinear dynamic controller is required.

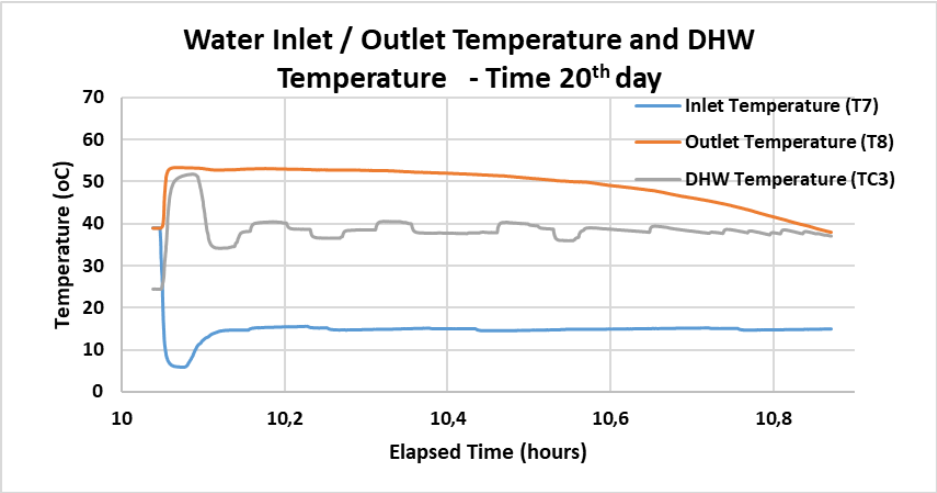

Figure 14 Water inlet/outlet and DHW temperature versus time graph for the 20th day of operation.

4. Conclusions

In this study, a linear controller for a latent solar thermal system was designed and implemented. The linear nature of the controller leads to a simple implementation, and the self-learning routine enhances the functionality and energy efficiency of the system. The solar kit controller was tested under real-world operating conditions. The results revealed that the training algorithms operate as designed and successfully improve the control equations. The controller exhibited improved behavior as the training progressed through the operating days. After the 20th day, the controller was fully trained, and no significant improvements in its operation were expected. The control routine for the charging of the system did not function properly when the controller was not trained. The flow of the HTF was controlled using the on/off approach because the partial overcast conditions at the testing area were not considered by the control routine. After the training was completed, the HTF flow was well regulated and followed the total and partial overcast conditions that occurred at the testing area. The temperature difference between the inlet and outlet of the HTF to the PCM tank was maintained at 5°C during the charging cycle. At dawn and dusk, when solar irradiance was low, the temperature difference in the charging circuit could not be maintained at 5°C, but the controller reduced the HTF flow to maintain the system in operation with an effective temperature difference (2°C). The performance of the controller on the 20th day was not ideal, especially for the stabilization of the DHW temperature. At the start of each DHW use cycle, the temperature of the water was stabilized after a considerable amount of time, resulting in energy

loss. During use, the DHW temperature was stabilized within acceptable limits. In particular, with the controller not trained, the temperature of the DHW at the start of the cycle matched the PCM tank temperature. With the cycle progressing, the temperature of the DHW could not be regulated well; it followed the tank's temperature with the same slope and stabilized at 38°C, which is the control limit for the DHW temperature. When the controller was fully trained (after 20 cycles), the initial stabilization time for DHW temperature was approximately 5 min. The output was well regulated within the range of 37°C–40°C. To further improve the performance of the proposed system, more sophisticated nonlinear control algorithms can be used at the expense of increased complexity and increased computational resources.

Author Contributions

Conceptualization, M.Gr.V., Y.C., M.K. J.K.; methodology, M.Gr.V., J.K., M.K; software, J.K.; formal analysis, J.K.; investigation, All; writing—original draft preparation, J.K., C.P., M.K.; writing—review and editing, J.K., M.K.; supervision, M.Gr.V., Y.C.; project administration, M.Gr.V., M.K.; funding acquisition, M.Gr.V., Y.C., M.K..

Funding

This research has been cofinanced by the European Regional Development Fund of the European Union and Greek national funds through the Operational Program Competitiveness, Entrepreneurship and Innovation, under the call RESEARCH _ CREATE _ INNOVATE (project code: T1EDK _01898).

Competing Interests

The authors have declared that no competing interests exist.

References

1. Douvi E, Pagkalos C, Dogkas G, Koukou MK, Stathopoulos VN, Caouris Y, et al. Phase change materials in solar domestic hot water systems: A review. Int J Thermofluids. 2021; 10: 100075.
2. Thakur A, Kumar R, Kumar S, Kumar P. Review of developments on flat plate solar collectors for heat transfer enhancements using phase change materials and reflectors. Mater Today Proc. 2021; 45: 5449-5455.
3. Dogkas G, Konstantaras J, Koukou MK, Vrachopoulos MG, Pagkalos C, Stathopoulos VN, et al. Development and experimental testing of a compact thermal energy storage tank using paraffin targeting domestic hot water production needs. Therm Sci Eng Prog. 2020; 19: 100573.
4. Dogkas G, Koukou MK, Konstantaras J, Pagkalos C, Lymperis K, Stathopoulos V, et al. Investigating the performance of a thermal energy storage unit with paraffin as phase change material, targeting buildings' cooling needs: An experimental approach. Int J Thermofluids. 2020; 3: 100027.
5. Koukou MK, Dogkas G, Vrachopoulos MG, Konstantaras J, Pagkalos C, Stathopoulos VN, et al. Experimental assessment of a full scale prototype thermal energy storage tank using paraffin for space heating application. Int J Thermofluids. 2020; 1: 100003.

6. Abdulmunem AR, Samin PM, Rahman HA, Hussien HA, Mazali II, Ghazali H. Numerical and experimental analysis of the tilt angle's effects on the characteristics of the melting process of pcm-based as PV cell's backside heat sink. Renew Energ. 2021; 173: 520-530.
7. Abdulmunem AR, Samin PM, Rahman HA, Hussien HA, Mazali II. Enhancing PV cell's electrical efficiency using phase change material with copper foam matrix and multi-walled carbon nanotubes as passive cooling method. Renew Energ. 2020; 160: 663-675.
8. Abdulmunem AR, Samin PM, Rahman HA, Hussien HA, Ghazali H. A novel thermal regulation method for photovoltaic panels using porous metals filled with phase change material and nanoparticle additives. J Energy Storage. 2021; 39: 102621.
9. Abdulmunem AR, Samin PM, Rahman HA, Hussien HA, Mazali II, Ghazali H. Experimental and numerical investigations on the effects of different tilt angles on the phase change material melting process in a rectangular container. J Energy Storage. 2020; 32: 101914.
10. Abdelsalam MY, Teamah HM, Lightstone MF, Cotton JS. Hybrid thermal energy storage with phase change materials for solar domestic hot water applications: Direct versus indirect heat exchange systems. Renew Energ. 2020; 147: 77-88.
11. De Andrade GA, Álvarez JD, Pagano DJ, Berenguel M. Nonlinear controllers for solar thermal plants: A comparative study. Control Eng Pract. 2015; 43: 12-20.
12. Badescu V. Optimal control of flow in solar collectors for maximum exergy extraction. Int J Heat Mass Transfer. 2007; 50: 4311-4322.
13. Badescu V. Optimal control of flow in solar collector systems with fully mixed water storage tanks. Energy Convers Manage. 2008; 49: 169-184.
14. de Araújo Elias T, da Costa Mendes PR, Normey-Rico JE. Hybrid predictive controller for overheating prevention of solar collectors. Renew Energ. 2019; 136: 535-547.
15. Víg P, Seres I, Vladár P. Improving efficiency of domestic solar thermal systems by a flow control. Sol Energy. 2021; 230: 779-790.
16. Araújo A, Pereira V. Solar thermal modeling for rapid estimation of auxiliary energy requirements in domestic hot water production: On-off flow rate control. Energy. 2017; 119: 637-651.
17. Araújo A, Pereira V. Solar thermal modeling for rapid estimation of auxiliary energy requirements in domestic hot water production: Proportional flow rate control. Energy. 2017; 138: 668-681.
18. Araújo A, Silva R, Pereira V. Solar thermal modeling for rapid estimation of auxiliary energy requirements in domestic hot water production: On-off versus proportional flow rate control. Sol Energy. 2019; 177: 68-79.
19. Tourou P, Konstantaras J, Vrachopoulos MG, Sourkounis C, Koukou MK, Pagkalos C, et al. Validation of a control algorithm for the efficient charging of PCM energy storage tanks using an emulation platform. Proceedings of the 8th International Conference ENERGY in BUILDINGS 2019; 2019 September 28; Athens, Greece. Atlanta: ASHRAE. DOI: 10.5281/zenodo.3564644.
20. Koukou MK, Konstantaras J, Dogkas G, Lymperis K, Stathopoulos VN, Vrachopoulos MG, et al. Development of a novel compact flat-plate solar collector integrated with thermal energy storage: Experimental evaluation of the energy stored under outdoors conditions. Proceedings of the 13th International Conference on Sustainable Energy & Environmental Protection; 2021 September 13-16; Vienna, Austria. ISBN: 978-3-900932-87-9.

21. Koukou MK, Pagkalos C, Dogkas G, Vrachopoulos MG, Douvi E, Caouris YG, et al. Computational approach of charging and discharging phases in a novel compact solar collector with integrated thermal energy storage tank: Study of different phase change materials. Energies. 2022; 15: 1113.

Enjoy *JEPT* by:

1. Submitting a manuscript
2. Joining in volunteer reviewer bank
3. Joining Editorial Board
4. Guest editing a special issue

For more details, please visit:
http://www.lidsen.com/journal/jept